DOI: 10.3901/CJME.2013.06.1091, available online at www.springerlink.com; www.cjmenet.com; www.cjmenet.com.cn

Modeling and Evaluating of Surface Roughness Prediction in Micro-grinding on Soda-lime Glass Considering Tool Characterization

CHENG Jun*, GONG Yadong, and WANG Jinsheng

School of Mechanical Engineering and Automation, Northeastern University, Shenyang 100004, China

Received September 12, 2012; revised August 5, 2013; accepted August 22, 2013

Abstract: The current research of micro-grinding mainly focuses on the optimal processing technology for different materials. However, the material removal mechanism in micro-grinding is the base of achieving high quality processing surface. Therefore, a novel method for predicting surface roughness in micro-grinding of hard brittle materials considering micro-grinding tool grains protrusion topography is proposed in this paper. The differences of material removal mechanism between convention grinding process and micro-grinding process are analyzed. Topography characterization has been done on micro-grinding tools which are fabricated by electroplating. Models of grain density generation and grain interval are built, and new predicting model of micro-grinding surface roughness is developed. In order to verify the precision and application effect of the surface roughness prediction model proposed, a micro-grinding orthogonally experiment on soda-lime glass is designed and conducted. A series of micro-machining surfaces which are 78 nm to 0.98 μm roughness of brittle material is achieved. It is found that experimental roughness results and the predicting roughness data have an evident coincidence, and the component variable of describing the size effects in predicting model is calculated to be 1.5×10^7 by reverse method based on the experimental results. The proposed model builds a set of distribution to consider grains distribution densities in different protrusion heights. Finally, the characterization of micro-grinding tools which are used in the experiment has been done based on the distribution set. It is concluded that there is a significant coincidence between surface prediction data from the proposed model and measurements from experiment results. Therefore, the effectiveness of the model is demonstrated. This paper proposes a novel method for predicting surface roughness in micro-grinding of hard brittle materials considering micro-grinding tool grains protrusion topography, which would provide significant research theory and experimental reference of material removal mechanism in micro-grinding of soda-lime glass.

Key words: micro-grinding, tool topography characterization, soda-lime glass, surface roughness prediction

1 Introduction

Micro products are applied widely in many fields and industries including telecommunications, portable consumer electronics, defense and biomedical engineering[1]. Micromachining has been carried out to satisfy the requirements for micro structured elements manufacturing which is growing fast[2].

Micro-grinding is a method to process the topography of work piece by using tool whose diameter is less than 1 mm. It could solve problems which are caused in process of micro-milling, and then catch much concern[3] as a result. Micro-grinding is also one of primary current high precision process methods of machining hard brittle material in micro-scale. Researchers have got some achievements in micro-grinding field. MORGAN, et al[4], did a micro-grinding experiment on tungsten carbide and achieved a 5.1 nm roughness surface, it is demonstrated that micro-grinding is a proper process method to improve surface quality of hard brittle and difficult to cut material, such as glass, tungsten carbide, etc. AURICH[5] fabricated a series of micro-grinding tool whose diameter are between 13 μm to 100 μm. He also focused on how to process complex micro structure of brittle material by micro-grinding, finally achieved a 10 nm roughness surface which was the most precision surface in worldwide. ZHANG[6] achieved a 60 nm roughness surface in micro-grinding nano-structured material coatings whose H_v is 12.5 GPa, provided a new research direction of micro-grinding. SHUN[7] used complex technology to fabricate diamond micro-grinding tools whose diameter is 100 μm, he focused on micro-grinding of ZrO_2 ceramic material and finally achieved a 0.085 μm roughness surface. CHENG, et al[8], built a material removal model in micro-grinding of hard brittle materials. The ductile-regime characters in micro-grinding of soda-lime glass were also investigated by CHENG[9], he proposed a complex model to define the critical condition of ductile-regime in

* Corresponding author. E-mail: jcheng@mail.neu.edu.cn
This project is supported by National Natural Science Foundation for Young Scholars of China(Grant No. 51205053), and National Natural Science Foundation of China(Grant No. 51075064)

micro-grinding and verified it in experiments.

Researchers mostly focused on the optimal process parameters of micro-grinding, but didn't give enough concern to systemically analyze surface formation mechanism.

This paper proposes a new method of micro-grinding surface roughness predicting. A predicting model which focuses on topography characterization of micro-grinding tool is developed considering the differences between convention grinding and micro-grinding process. The process chain for micro-grinding research work of this paper is shown in Fig. 1.

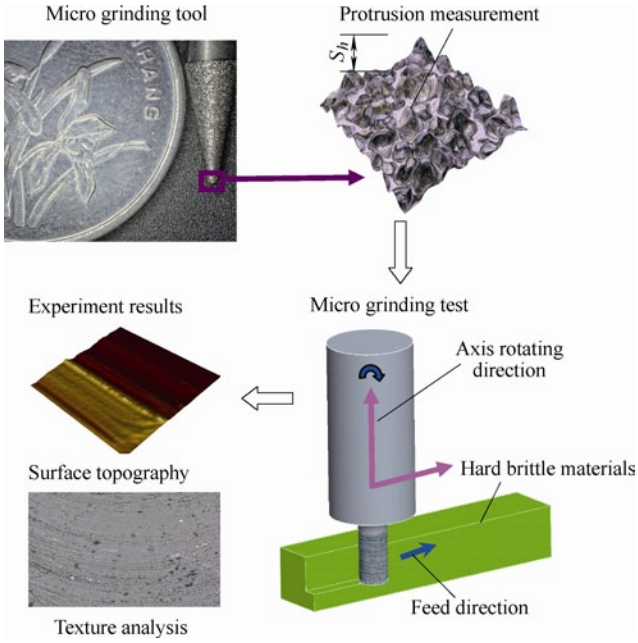

Fig. 1. Micro grinding research concept

In order to verify the predicting model of micro-grinding surface roughness which is developed in this paper, a micro-grinding orthogonally experiment on soda-lime glass has been designed and conducted on a micro-desktop. This micro-desktop which is developed by WANG[10] has a 160 kr/min maximum speed V_s of its axis.

2 Micro-grinding Tool Measurement

The topographical analysis on diamond tool has important significance to surface prediction of diamond grinding wheel. XIE, et al[11], did the tool topography measurement by using various measuring instruments, he gave a conclusion that 3D-graphical evaluation of micro-scale protrusion is applicable. The method of micro-grinding surface roughness prediction is also based on graphical evaluation data. ZHOU, et al[12], proposed and developed a method for predicting the surface roughness of grinding work piece by simulation verification without experiment.

In this paper, an equipment is used to measure and take the grain protrusions of micro-grinding tool based on focus-depth method, it is shown in Fig. 2(a). Fig. 2(b) shows the grain protrusions in 1 000 scale magnify.

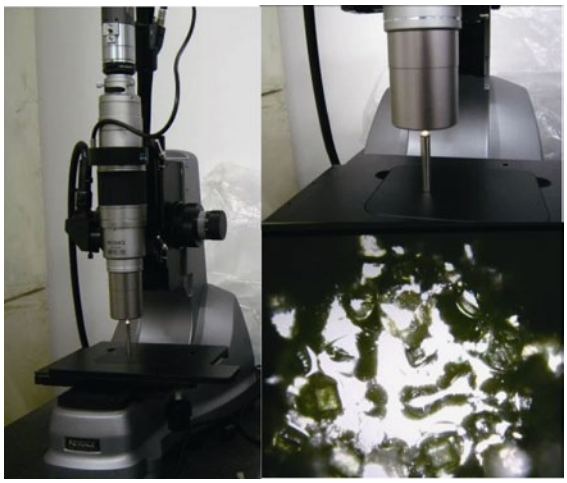

(a) Microscope and image system

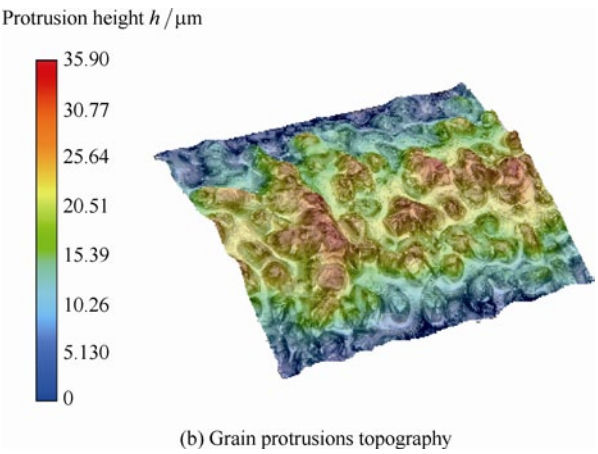

(b) Grain protrusions topography

Fig. 2. Measurement of micro-grinding tool

3 Tool Topography Characterization

In grinding tool characterization research field, YAN, et al[13], focused on alumina grinding wheel, and imported Birmingham function to evaluate surface topography of alumina grinding wheels. It was found that protrusion heights of alumina grinding wheels are according with normal distribution. XIE, et al[11], characterized the micro-grit protrusion in hard brittle material grinding, then gave a conclusion that GT-truncation increases active grain number and grain protrusion angle in ductile-mode grinding.

3.1 Grain density generation

Micro-grinding tool which is shown in Fig. 2 is fabricated by diamond electroplating. It could be assumed that grits are arranged by the same distance L along circle direction in the ideal condition. But grits distance is not regular arranged on real micro-grinding tool surface, and grains are usually randomly distributed on micro-grinding tool surface.

The grains also have different terms of sizes, shapes,

distribution densities and orientations. Therefore, there must be different grain densities at different protrusion heights.

Eq. (1) is an equation proposed by NGUYEN, et al[14], it provided a criterion for selecting the optimal sampling interval:

$$S_{ds} = \frac{n_s}{(M-1)(N-1)\Delta x \Delta y}, \tag{1}$$

where n_s—Number of summits,
M—Number of data points along x direction,
N—Number of data points along y direction,
Δx—Sampling interval along x direction,
Δy—Sampling interval along y direction.

Fig. 3 shows how to get the acquisition of grains at different sampling intervals.

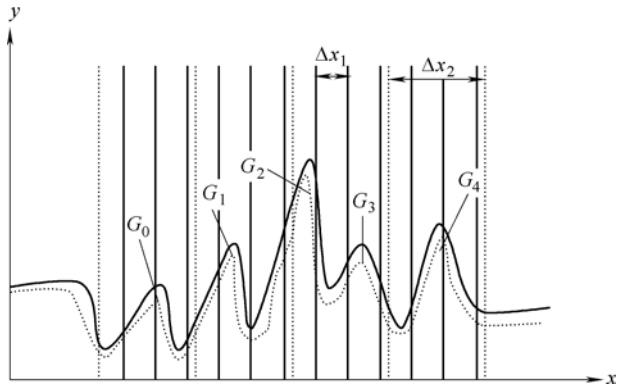

Fig. 3. Distribution density of different sampling intervals

As it is mentioned above, grains on micro grinding tool are distributed randomly. Grains densities are different at different protrusion heights as Fig. 4 shows, such as h_1 and h_2. Therefore, this paper develops a new model which Eq. (2) shows to character grains densities at different protrusion heights. This model considers grains distribution densities at different protrusion heights by building a set of distribution $\{S_h\}$, the density could be described as Eq. (3) at a protrusion height h. The comparison with average grain distribution density also could be calculated and indicated as Eq. (4). Fig. 5 shows the characterization of diamond micro-grinding tool which is used in experiment of this paper.

$$\{S_h\} = \{S_{h1}, S_{h2}, S_{h3}, \cdots, S_{h(n-1)}, S_{hn}\}, \tag{2}$$

$$S_{hn} = \frac{n_h}{(M_h-1)(N_h-1)\Delta x_h \Delta y_h}, \tag{3}$$

$$\rho_h = \frac{S_{hn}}{S_{ds}}, \tag{4}$$

where n_h—Number of summits at h height,
M_h—Number of data points along x direction at h height,
N_h—Number of data points along y direction at h height,
Δx_h—Sampling interval along x direction at h height,
Δy_h—Sampling interval along y direction at h height.

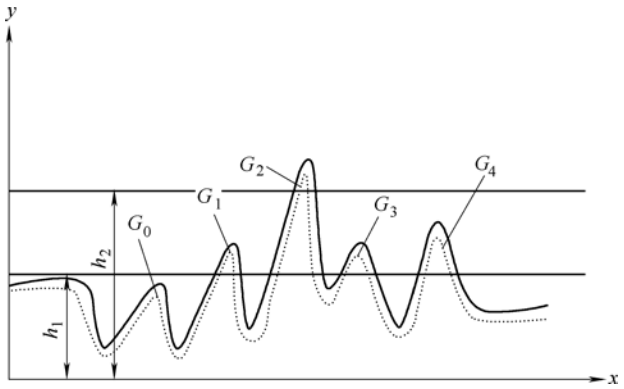

Fig. 4. Distribution densities at different grain protrusion heights

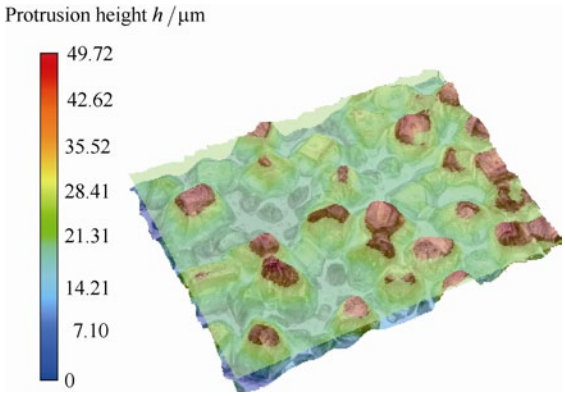

Fig. 5. Characterization of micro-grinding tool grains densities in different protrusion heights

3.2 Grain interval generation

Micro-grinding tool this paper used is fabricated by electroplate, MALKIN[15] gave the expression of grain dimension d_g by a simply way that building the relationship between grain size and aperture of sieve. ZHOU, et al[12], also used this method to build a grinding surface roughness predicting model, they made a test with conventional grinding process but without experimental verify. Eq. (5) shows the relationship between the max grain dimension d_{gmax} and grain particle size:

$$d_{g\max}(\text{mm}) = 15.2M^{-1}, \tag{5}$$

where M is the grains' particle size number, then the average grain dimension could be deduced and shown as Eq. (6):

$$d_{gavg}(\text{mm}) = 68M^{-1.4}. \tag{6}$$

HWANG[16] gave a conclusion that the grain protrusion height is found to obey Gaussian distribution, the relationship between its mean value h_{avg} and standard deviation σ is shown as Eq. (7) and Eq. (8):

$$\mu = d_{\text{gavg}}, \tag{7}$$

$$\sigma = \frac{d_{\text{g max}} - d_{\text{gavg}}}{3}. \tag{8}$$

Grain interval indicates the distance between two adjacent grains, it is an important parameter for generating a micro-grinding tool topography. MALKIN[15] proposed that it had a relationship with the structure number S of the grinding wheel. S indicates the volumetric concentration of grains, and volume number of the wheel V_g could be shown as Eq. (9):

$$V_g = 2(32 - S). \tag{9}$$

Assuming that grains distribute on wheel surface uniformly, the relationship could be indicated as Eq. (10)[17]:

$$\frac{\pi}{6} d_{\text{gavg}}^3 = V_g \Delta^3. \tag{10}$$

Then the grain interval Δ could be derived and shown as Eq. (11):

$$\Delta = 137.9 M^{-1.4} \sqrt[3]{\frac{\pi}{32 - S}}. \tag{11}$$

Considering the different protrusion effects which are proposed in Eqs. (2)–(4), the micro-grinding tool's grain interval Δ_h at different protrusion heights finally could be indicated as Eq. (12):

$$\Delta_h = \rho_h \Delta = \frac{137.9 S_{hn} M^{-1.4}}{S_{\text{ds}}} \sqrt[3]{\frac{\pi}{32 - S}}. \tag{12}$$

4 Prediction Model Development

4.1 Material removal process analysis

Conventional grinding speed v_s could be calculated as Eq. (13):

$$v_s = \frac{\pi D n}{60}, \tag{13}$$

where n—Wheel speed (r/min),
D—Wheel diameter (m)

Fig. 6 shows the grit movement along work piece's surface and the grinding path of single grit in conventional grinding[15]. Previous grit's cutting path AA' equals to s, s is also the work piece's movement during time of two adjacent grits cutting. It could be expressed as Eq. (14), in which L is the distance between two adjacent grits, v_w is work piece's feed rate speed:

$$s = \frac{L v_w}{v_s}. \tag{14}$$

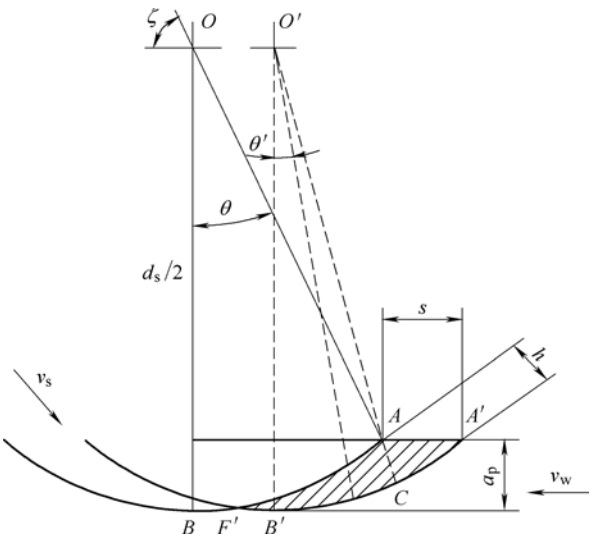

Fig. 6. Undeformed chip thickness of conventional grinding

The undeformed chip thickness h_m equals to the length of AC in Fig. 6, it could be expressed as Eq. (15), where d_s is wheel diameter:

$$h_m = O'C - O'A = \frac{d_s}{2} - O'A. \tag{15}$$

In $\triangle OO'C$, length of $O'A$ could be expressed as Eq. (16):

$$O'A = \left[\left(\frac{d_s}{2} \right)^2 + s^2 - s d_s \cos\xi \right]^{1/2}, \tag{16}$$

and it also could be derived as

$$O'A = \left[\left(\frac{d_s}{2} \right)^2 + s^2 - s d_s (1 - \cos^2\theta)^{1/2} \right]^{1/2}, \tag{17}$$

$$\cos\theta = 1 - \frac{2a_p}{d_s}. \tag{18}$$

Eq. (18) shows the relationship between d_s and grinding depth a_p. The undeformed chip thickness in conventional grinding process could be finally expressed as Eq. (19) by taking Eqs. (17), (18) into Eq. (15):

$$h_m = 2s \left(\frac{a_p}{d_s} \right)^{1/2} - \frac{s^2}{d_s}. \tag{19}$$

Conventional grinding process and micro-grinding process are shown in Fig. 7. Obviously, Eq. (19) is a conclusion which is derived by considering that a_p/d_s is far less than 1. Although the wheel diameter d_s is larger than grinding depth a_p in conventional grinding process indeed,

the tool diameter in micro-grinding process is almost less than 1 mm, and new developed micro-grinding tool's minimum dimension is close to micrometer scale[15].

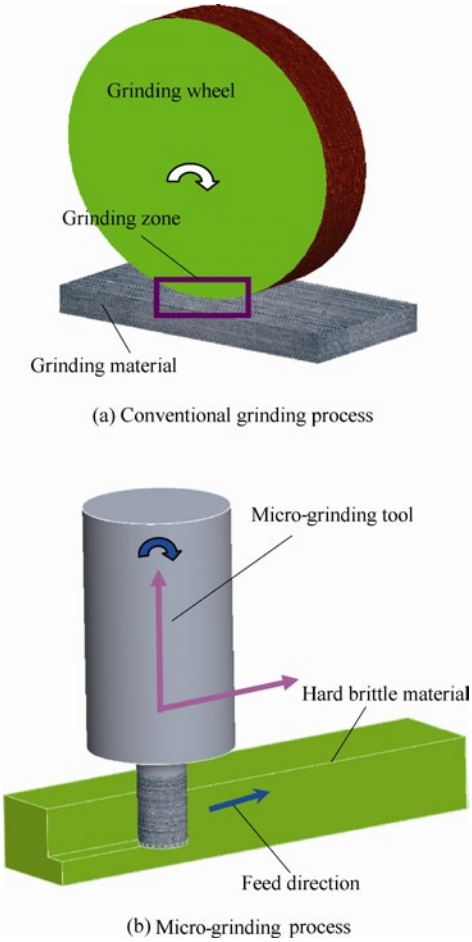

Fig. 7. Conventional grinding and micro-grinding process

In this condition, tool sometimes cuts within material's crystal particles during micro-grinding process. Considering the effects of minimum chip thickness, micro size effects, the material removal mechanism could present significant differences comparing with conventional machining[18]. Therefore, the processing model of micro-grinding must consider tool diameter and size effect in micro scale. The undeformed chip thickness h_m in micro-grinding process is shown as Fig. 8.

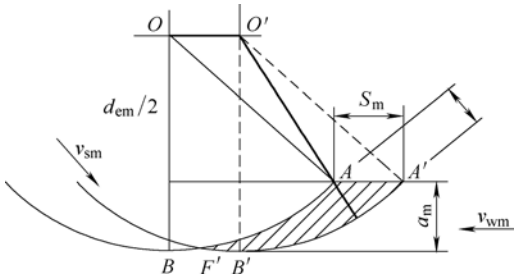

Fig. 8. Undeformed chip thickness of micro-grinding

The undeformed chip thickness of micro-grinding h_m could be expressed as Eq. (20). This model considers the relation between d_s and a_p in micro-grinding process.

$$h_m = 2s\left(\frac{a_m}{d_s}\right)^{1/2}\left(1-\frac{a_m}{d_s}\right)^{1/2} - \frac{s^2}{d_s}. \tag{20}$$

Meanwhile, this paper proposes a component variable M_d to describe the effects of micro scale grinding, then the h_m could be expressed as Eq. (21):

$$h_m = M_d\left[2s\left(\frac{a_m}{d_s}\right)^{1/2}\left(1-\frac{a_m}{d_s}\right)^{1/2} - \frac{s^2}{d_s}\right]. \tag{21}$$

Subsequently, by substituting Eq. (14) into Eq. (21), the undeformed chip thickness model of micro-grinding h_m finally could be achieved and shown as Eq. (22):

$$h_m = M_d\left[2\left(\frac{Lv_w}{v_s}\right)\left(\frac{a_m}{d_s}\right)^{1/2}\left(1-\frac{a_m}{d_s}\right)^{1/2} - \frac{L^2}{d_s}\left(\frac{v_w}{v_s}\right)^2\right]. \tag{22}$$

4.2 Surface roughness R_a modeling

This paper develops a new predicting model of surface roughness during micro-grinding process. Fig. 9 shows the surface formation mechanism and surface roughness R_t of micro-grinding process. The angle α could be ignored because it is near to zero in conventional grinding process. But the micro-grinding tool diameter is much small, and the value of v_w/v_g also changes largely in micro-grinding process. Therefore, angle α must be considered as a critical component of roughness equation in micro-grinding process.

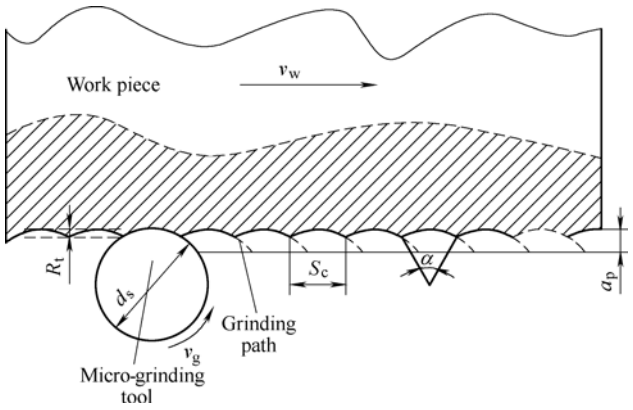

Fig. 9. Surface texture and roughness in micro-grinding process

Roughness R_t shown in Fig. 9 can be calculated as

$$R_t = \frac{1}{2}d_s\left(1-\cos\frac{\alpha}{2}\right), \tag{23}$$

and it also could be simply described as

$$R_t = d_s\sin^2\frac{\alpha}{4}. \tag{24}$$

Angle α could be ignored in conventional process, and

considering the equations which are shown as below:

$$\sin\frac{\alpha}{2}=\sin\frac{\alpha}{4},\quad \sin\frac{\alpha}{2}=\frac{s_c}{d_s},$$

R_t could be deduced as Eq. (25):

$$R_t=\frac{{s_c}^2}{4d_s}, \tag{25}$$

s_c in Eq. (25) is substituted by Eq. (14), then R_t could be shown as Eq. (26)[12]:

$$R_t=\frac{1}{4}\left(\frac{v_w L}{v_s d_s^{1/2}}\right)^2. \tag{26}$$

As it is discussed before, the angle α mustn't be ignored in micro-grinding process, or it would cause large error. Therefore, this paper considered angle α and micro size effects, then proposed a component variable M_r to describe the effects of micro scale. Then R_t in micro-grinding could be expressed as Eq. (27):

$$R_t=\frac{1}{2}M_r d_s\left(1-\cos\frac{\alpha}{2}\right), \tag{27}$$

where $\cos\dfrac{\alpha}{2}=\left(1-\sin^2\dfrac{\alpha}{2}\right)^{1/2}=\left(1-\dfrac{s_c^2}{d_s^2}\right)^{1/2}$.

s_c in Eq. (27) is substituted by Eq. (14), the roughness model of micro-grinding R_t could be deduced and shown as Eq. (28):

$$R_t=\frac{1}{2}M_r\left\{d_s-\left[d_s^2-\left(\frac{v_w L}{v_s}\right)^2\right]^{1/2}\right\}. \tag{28}$$

With considering the grains distribution densities at different protrusion heights which has been proposed in Eqs. (1), (3), finally the prediction model of micro-grinding surface roughness R_h could be achieved and shown as follows:

$$L_h=\Delta_h, \tag{29}$$

$$R_h=\frac{1}{2}M_r d_s-\frac{1}{2}M_r\cdot \left\{d_s^2-\left[\frac{137.9 v_w n_h M^{-1.4}(M-1)(N-1)\Delta x\Delta y}{v_s n(M_h-1)(N_h-1)\Delta x_h\Delta y_h}\sqrt[3]{\frac{\pi}{32-S}}\right]^2\right\}^{1/2}. \tag{30}$$

5 Experiment Setup

Fig. 10 shows the situation of soda-lime glass micro-grinding process. Equipments and micro-grinding tool which have been used in experiments are shown in Fig. 10.

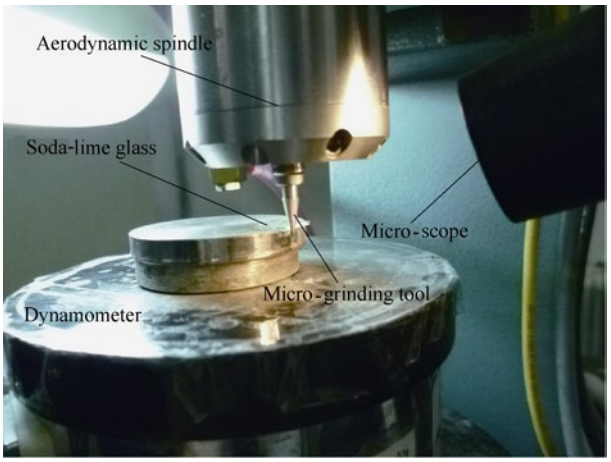

Fig. 10. Micro-grinding experiment equipments and process

Soda-lime glass (a product of Corning company) is chosen to be experiment material. Table 1 shows its properties.

Table 1. Basic attributes of Soda-lime glass

Parameter	Value
Coefficient of thermal expansion β/(m • K^{-1})	85
Strain point T_1/℃	506
Annealing point T_2/℃	545
Softening point T_3/℃	726
Density ρ/ (kg • m^{-3})	2.49
Modulus of elasticity E/ (kg • mm^{-2})	7.04

The experiment is designed with different levels and factors. Table 2 shows the experimental parameters such as f_z(feed rate), a_p (grinding depth), v_g(grinding speed). f_z is set between 100 μm/s to 500 μm/s, a_p is set between 10 μm to 30 μm, v_g is set between 35 kr/min to 120 kr/min.

Table 2. Experiment factors and levels of micro-grinding on soda-lime glass

Factor	Level				
	1	2	3	4	5
Grinding feed rate f_z /(μm • s^{-1})	100	200	300	400	500
Grinding depth a_p /μm	10	15	20	25	30
Rotate speed v_g/(kr • min^{-1})	35	50	75	100	120

6 Results and Discussion

Fig. 11 shows several micro-grinding slots and surface topography measurements which are the results of soda-lime glass micro-grinding experiment. It turns out that there is the same format grinding texture in micro-grinding and conventional grinding of soda-lime glass.

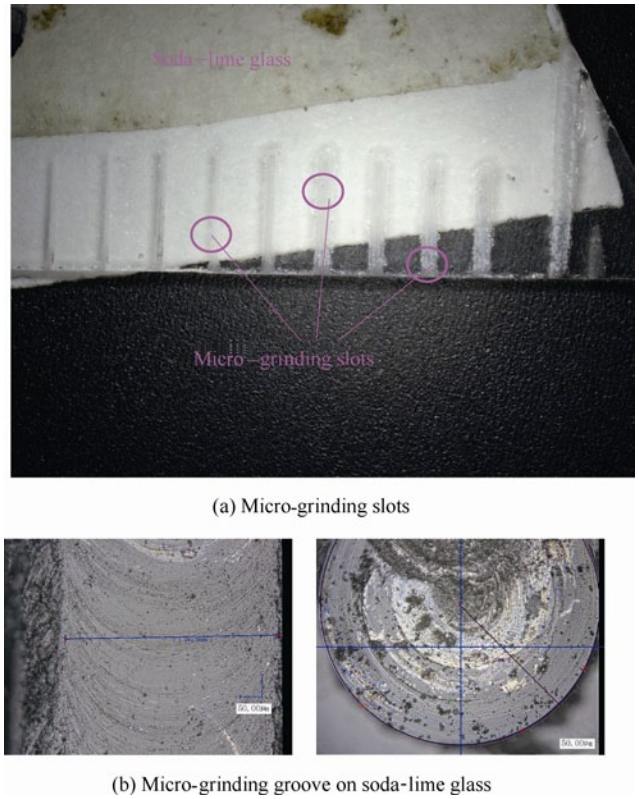

(a) Micro-grinding slots

(b) Micro-grinding groove on soda-lime glass

Fig. 11. Micro-grinding slots on soda-lime glass

Fig. 12 shows the surface topography measurements of micro-grinding results. Figs. 12(a), 12(b), 12(c) all have large brittle grooves on surface, but Fig. 12(d) doesn't have.

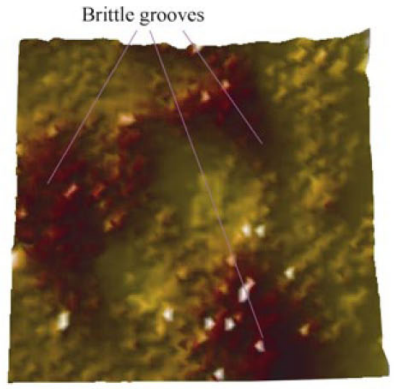

(a) f_z=500 μm/s, a_p=20 μm, v_g=35 kr/min, R_a=2.47 μm

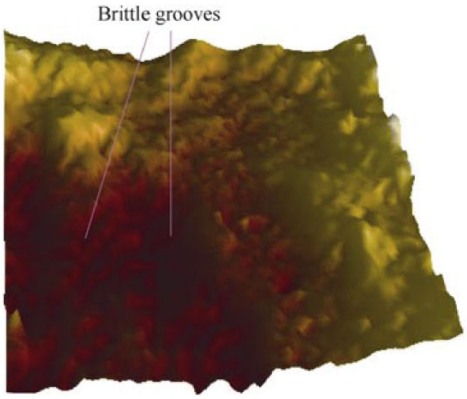

(b) f_z=300 μm/s, a_p=20 μm, v_g=75 kr/min, R_a=0.723 μm

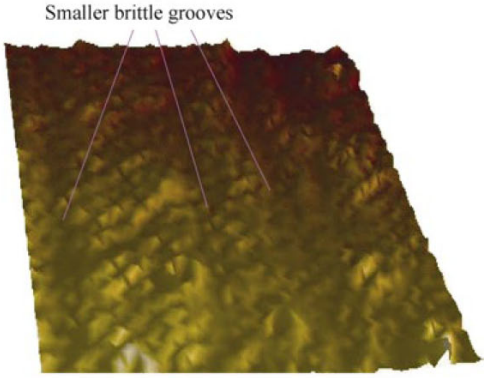

(c) f_z=200 μm/s, a_p=15 μm, v_g=50 kr/min, R_a=0.415 μm

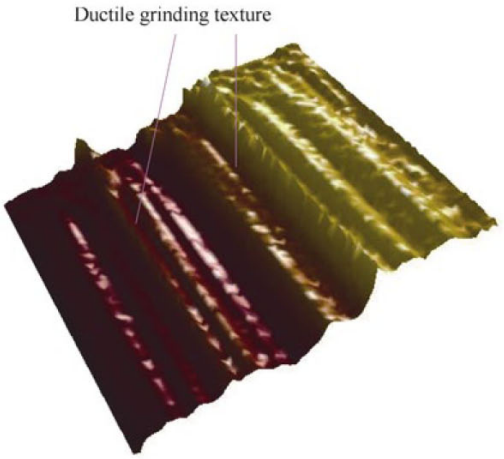

(d) f_z=100 μm/s, a_p=30 μm, v_g=10 kr/min, R_a=56 nm

Fig. 12. Surface topography of soda-lime glass in micro-grinding

The relationships between roughness and parameters such as grinding speed, feed rate and grinding depth are shown in Fig. 13. Roughness increases 312% when feed rate increases from 100 μm to 500 μm, roughness decreases 70.5% when grinding speed increases from 35 kr/min to 120 kr/min. Results of experiments indicate that low feed rate and high tool rotation speed could achieve a low R_a value, and micro-grinding depth a_p doesn't show a regular effect to surface roughness.

7 Prediction of Surface Roughness

Tables 3–7 show experimental results of micro-grinding surface roughness and the predicting model results. R_a(E) is the experimental results and R_a(P) is the predicting data. M_d in predicting model is supposed to be 1.5×10^7, the predicting results could be more accurate than conventional method. Its error is 1×10^{24} magnitude comparing with the results this paper proposes.

Fig. 14 shows a comparison between two groups of surface roughness data in micro-grinding process with different micro-grinding depth. Predicting results are deduced by Eq. (29) considering different grain densities.

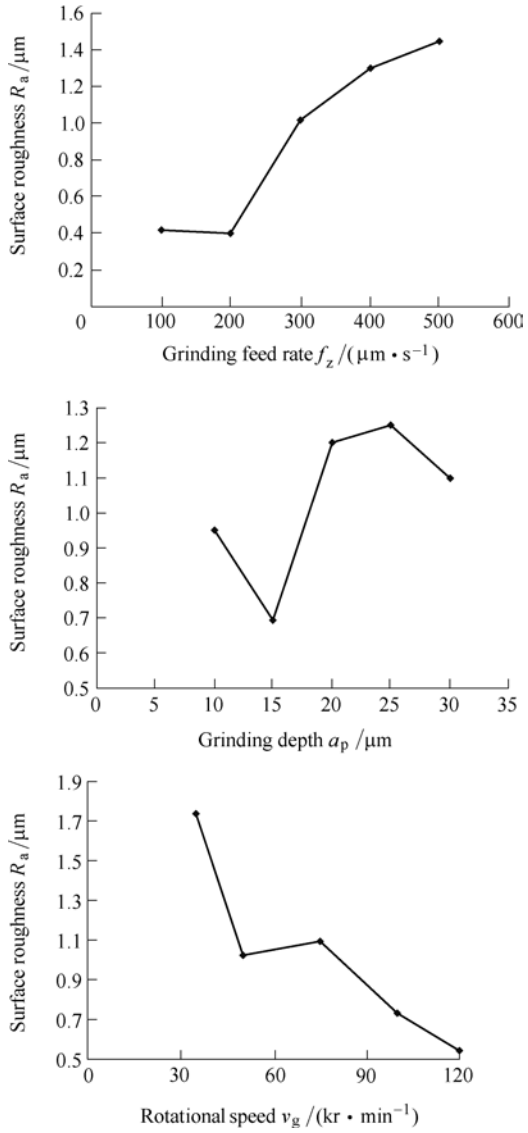

Fig. 13. Relation between roughness and effects

Table 3. Experiment result and prediction data (a_p=10 μm)

No.	Grinding depth a_p/μm	Grinding feed rate f_z /(μm • s^{-1})	Rotational speed v_g/(kr • min^{-1})	Experimental roughness result R_a(E)/μm	Model predicting roughness result R_a(P)/μm
1	10	100	35	0.59	0.284
2	10	200	75	0.553	0.096
3	10	300	120	0.666	0.314
4	10	400	50	1.124	0.992
5	10	500	100	2.88	3.489

Table 4. Experiment result and prediction data (a_p=15 μm)

No.	Grinding depth a_p/μm	Grinding feed rate f_z /(μm • s^{-1})	Rotational speed v_g/(kr • min^{-1})	Experimental roughness result R_a(E)/μm	Model predicting roughness result R_a(P)/μm
1	15	100	75	0.105	0.062
2	15	200	50	0.415	0.558
3	15	300	35	1.71	2.563
4	15	400	120	0.521	0.387
5	15	500	100	0.731	0.872

Table 5. Experiment result and prediction data (a_p=20 μm)

No.	Grinding depth a_p/μm	Grinding feed rate f_z /(μm • s^{-1})	Rotational speed v_g/(kr • min^{-1})	Experimental roughness result R_a(E)/μm	Model predicting roughness result R_a(P)/μm
1	20	100	120	0.354	0.024 2
2	20	200	100	0.269	0.139 5
3	20	300	75	0.723	0.558 2
4	20	400	50	1.39	2.232
5	20	500	35	5.47	7.12

Table 6. Experiment result and prediction data (a_p=25 μm)

No.	Grinding depth a_p/μm	Grinding feed rate f_z /(μm • s^{-1})	Rotational speed v_g/(kr • min^{-1})	Experimental roughness result R_a(E)/μm	Model predicting roughness result R_a(P)/μm
1	25	100	50	0.202	0.139
2	25	200	35	0.958	1.139
3	25	300	120	0.277	0.218
4	25	400	100	0.657	0.558
5	25	500	75	1.95	1.55

Table 7. Experiment result and prediction data (a_p=30 μm)

No.	Grinding depth a_p/μm	Grinding feed rate f_z /(μm • s^{-1})	Rotational speed v_g/(kr • min^{-1})	Experimental roughness result R_a(E)/μm	Model predicting roughness result R_a(P)/μm
1	30	100	100	0.056	0.034
2	30	200	75	0.385	0.248
3	30	300	50	0.934	1.256
4	30	400	35	2.95	4.557
5	30	500	120	0.576	0.605

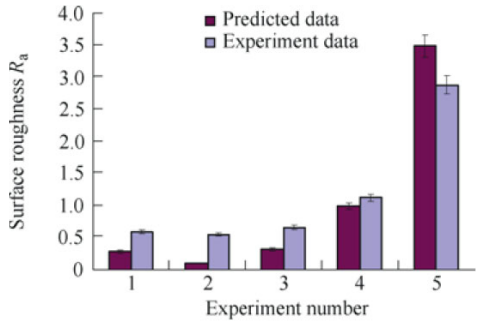

(a) a_p=10 μm

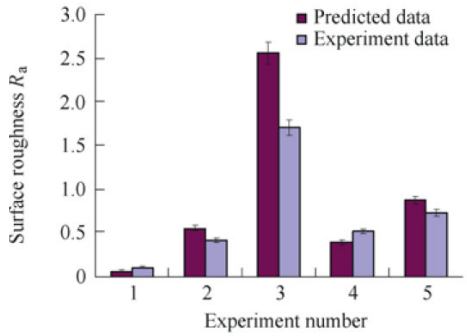

(b) a_p=15 μm

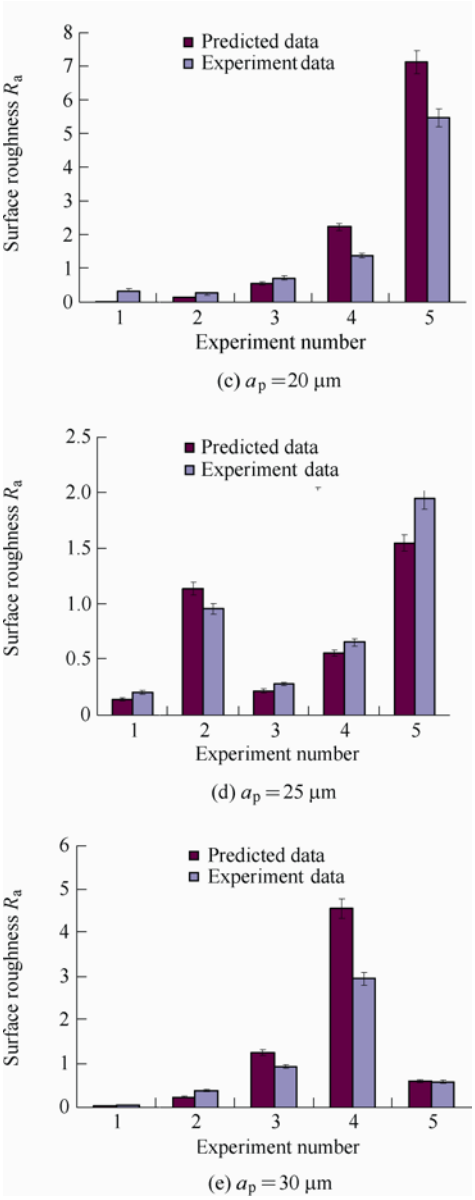

Fig. 14. Surface roughness comparison with different a_p in micro-grinding

8 Conclusions

(1) A new model of set $\{S_n\}$ for characterizing grains distribution densities of micro-grinding tool has been built. This model distinguishes the different densities at different protrusion heights by S_h.

(2) Grain interval Δ_h at different protrusion heights of micro-grinding tool has been calculated and derived. The ratio ρ_h of specific density to average grains distribution density has been considered.

(3) A new surface roughness prediction model of micro-grinding is developed in this paper. It could predict micro-grinding surface roughness considering characterization of micro-grinding tool. Undeformed chip thickness of micro-grinding and the differences in material removal mechanism to conventional grinding have been discussed. From the deviation comparison between experimental measurements and prediction results, it is found that the effectiveness of method this paper proposes has been proved.

(4) An orthogonally micro-grinding experiment on soda-lime glass has been designed and conducted. The relationships between roughness values and parameters such as grinding speed, feed rate, grinding depth have been revealed. Experimental results indicate that low feed rate and high grinding speed could achieve a precision R_a value. Micro-grinding depth doesn't show a clear law of function to surface quality.

References

[1] DORNFELD D, MIN S, TAKEUCHI Y. Recent advances in mechanical micromachining[J]. *Annals of the CIRP*, 2006, 55(2): 745–768.

[2] BRINKSMEIER E, GLABE R, OSMER J. Ultra-precision diamond cutting of steel molds[J]. *Annals of the CIRP*, 2006, 55(1): 551–554.

[3] SCHALLER T, BOHN L, MAYER J, et al. Microstructure grooves with a width of less than 50 mm cut with ground hard metal micro-end mills[J]. *Precision Engineering*, 1999, 23: 229–235.

[4] MORGAN C J, VALLANCE R R, MARSH E R. Specific grinding energy while microgrinding tungsten carbide with polycrystalline diamond micro tools[C/CD]//*ICOMM-2007 2nd International Conference on Micro-Manufacturing*, Sep 10 2007, Greenville, South Carolina, USA, No. 39.

[5] AURICH J C, ENGMANN J, SCHUELER G M, et al. Micro grinding tool for manufacture of complex structures in brittle materials[J]. *CIRP Annals-Manufacturing Technology*, 2009, 58(1): 311–314.

[6] ZHANG Bi, LIU X B, BROWN C. Microgrinding of nanostructured material coatings[J]. *Annals of the CIRP*, 2002, 51(1): 251–254.

[7] SHUN T C, TSAI M Y, LAI Y C, et al. Development of a micro diamond grinding tool by compound process[J]. *Journal of Materials Processing Technology*, 2009, 209: 4 698–4 703.

[8] CHENG Jun, GONG Yadong, WU Zhizheng, et al. Experimental study on mechanism of surface formation for micro-grinding of hard brittle material[J]. *Chinese Journal of Mechanical Engineering*, 2012, 48(21): 190–201. (in Chinese)

[9] CHENG Jun, GONG Yadong. Experimental study on ductile-regime micro-grinding character of soda-lime glass with diamond tool[J]. *International Journal of Advanced Manufacturing Technology*, 2013, 10.1007/ s00170-013-5000-3.

[10] WANG Jinsheng, GONG Yadong, ABBA G, et al. Chip formation analysis in micromilling operation[J]. *International Journal of Advanced Manufacturing Technology*, 2009, 45(5–6): 430.

[11] XIE Jin, LU Yongxian. Study on axial-feed mirror finishgrinding of hard and brittle materials in relation to micron-scale grain protrusion parameters[J]. *International Journal of Machine Tools and Manufacture*, 2011, 51(1): 84–93.

[12] ZHOU X, XI Feng. Modeling and predicting surface roughness of the grinding process[J]. *International Journal of Machine Tools & Manufacture*, 2002, 42(8): 969–977.

[13] YAN Lan, RONG Yiming, JIANG Feng. Quantitive evaluation and modeling of alumina grinding wheel surface topography[J]. *Chinese Journal of Mechanical Engineering*, 2011, 47(17): 179–186. (in Chinese)

[14] NGUYEN A T, BUTLER D L. Correlation of grinding wheel topography and grinding performance: A study from a viewpoint of three-dimensional surface characterisation[J]. *Journal of Materious Processing Technology*, 2008, 208(1–3): 14–23.

[15] MALKIN S. *Grinding technology theory and applications of machining with abrasives*[M]. Society of Manufacturing Engineers, Dearborn, MI, USA. 2002.

[16] HWANG T W, EVENS C J, MALKIN S. High speed grinding of silicon nitride with electroplated diamond wheels: part 1: wear and wheel life[J]. *ASME Journal of Manufacturing Science and Engineering*, 2000, 122: 32–41.
[17] CHEN X, ROWE W B. Analysis and simulation of the grinding process, part 1: generation of the grinding wheel surface[J]. *International Journal of Machine Tools & Manufacturing*, 1996, 36(8): 871–882.
[18] LAI Xinmin, LI Hongtao, LI Chengfeng, et al. Modeling and analysis of micro scale milling considering size effect, micro cutter edge radius and minimum chip thickness[J]. *International Journal of Machine Tools & Manufacture*, 2008, 48(1): 1–14.

Biographical notes

CHENG Jun, born in 1981, is currently an lecturer at *Northeastern University, China*. He received his PhD degree from *Northeastern University, China*, in 2011. His research interests include micro precision process, grinding mechanism.
Tel: +86-13998854728, +86-24-83687626;
E-mail: jcheng@mail.neu.edu.cn

GONG Yadong, born in 1958, is currently a professor and a PhD candidate supervisor at *Northeastern University, China.* His main research interests include grinding mechanism, digital manufacturing.
E-mail: gongyd@mail.neu.edu.cn

WANG Jinsheng, born in 1981, is currently a superviser of a diamond tool company. He received his PhD degree from *Northeastern University, China*, in 2009. His main research interests is micro precision machining.